# Transforming yeast peroxisomes into microfactories for the efficient production of high-value isoprenoids

Simon Dusséaux[a] , William Thomas Wajn[a] , Yixuan Liu[a] , Codruta Ignea[a,1] , and Sotirios C. Kampranis[a,2]

[a]Biochemical Engineering Group, Plant Biochemistry Section, Department of Plant and Environmental Sciences, University of Copenhagen, 1871 Frederiksberg C, Denmark

Current approaches for the production of high-value compounds in microorganisms mostly use the cytosol as a general reaction vessel. However, competing pathways and metabolic cross-talk frequently prevent efficient synthesis of target compounds in the cytosol. Eukaryotic cells control the complexity of their metabolism by harnessing organelles to insulate biochemical pathways. Inspired by this concept, herein we transform yeast peroxisomes into microfactories for geranyl diphosphate-derived compounds, focusing on monoterpenoids, monoterpene indole alkaloids, and cannabinoids. We introduce a complete mevalonate pathway in the peroxisome to convert acetyl-CoA to several commercially important monoterpenes and achieve up to 125-fold increase over cytosolic production. Furthermore, peroxisomal production improves subsequent decoration by cytochrome P450s, supporting efficient conversion of (S)-(−)-limonene to the menthol precursor *trans*-isopiperitenol. We also establish synthesis of 8-hydroxygeraniol, the precursor of monoterpene indole alkaloids, and cannabigerolic acid, the cannabinoid precursor. Our findings establish peroxisomal engineering as an efficient strategy for the production of isoprenoids.

metabolic engineering | synthetic biology | terpenoid | mevalonate pathway | compartmentalization

**M**ost metabolic engineering strategies for the production of valuable chemicals utilize the cytosol as a one-pot reaction vessel, where multiple enzymes are introduced to catalyze long reaction cascades (1). However, this approach frequently results in poor yields, formation of undesirable by-products, or toxicity (2, 3), because cellular metabolism is an intricate mesh of reactions involving extensive cross-talk and elaborate regulatory mechanisms. Living organisms have devised solutions to overcome similar challenges by confining pathways within intracellular compartments to streamline reaction cascades and shield intermediates from competing pathways (4). Thus, nature's compartmentalization strategy can provide inspiration for solving metabolic engineering challenges (5).

Monoterpenoids, monoterpene indole alkaloids, and cannabinoids are groups of specialized metabolites valued for their fragrant and therapeutic properties. Due to a sizeable and rapidly expanding world market [collectively currently exceeding 10 billion USD (6, 7)], sourcing these molecules from nature or deriving them from petrochemicals is no longer sustainable, prompting efforts for their production in engineered microorganisms (8–12). The biosynthesis of all these compound groups shares a common building block, the universal 10-carbon isoprenoid precursor geranyl diphosphate (GPP) (13). However, synthesis of GPP-derived compounds in the industrial workhorse *Saccharomyces cerevisiae* has been particularly challenging due to the difficulty in creating a sufficiently large pool of GPP (10). This is the result of a strong competition for GPP by the native sterol biosynthesis pathway (10), which is essential for growth (Fig. 1). In yeast, GPP is only synthesized as an intermediate en route to farnesyl diphosphate (FPP), the precursor of sterols, and no other yeast metabolite is produced from GPP. Yeast cells employ a highly efficient cytoplasmic enzyme, Erg20p, which

functions as a bifunctional synthase that condenses isopentenyl diphosphate (IPP) and dimethylallyl diphosphate (DMAPP) first to GPP and subsequently to FPP (Fig. 1). As a result, once synthesized, GPP is rapidly converted to FPP by Erg20p, not allowing high enough fluxes to heterologous pathways converting GPP to desirable high-value metabolites (10, 14). Although several innovative strategies have been employed to overcome this limitation, such as engineering Erg20p stability (15) and specificity (14), or establishment of an orthogonal pathway based on an isomeric substrate (10), synthesis of 10-carbon isoprenoids in yeast is still markedly less efficient than other isoprenoids, whose production has reached industrial levels (16–18). For example, the sesquiterpenes farnesene and amorphadiene are being produced in titers that exceed 134 g/L and 40 g/L, respectively, while the highest reported monoterpene titers in yeast currently do not exceed 0.9 g/L for limonene (19) and 1.68 g/L for geraniol (20).

The challenge faced in the production of GPP-derived compounds can be addressed by the same strategy used by eukaryotic cells to solve similar issues within their own metabolism. Organelles, such as mitochondria, plastids, and peroxisomes, are exploited to isolate intermediates from competing pathways, shield enzymes from inhibitors, and protect the rest of the cell from toxic compounds. Thus, an attractive alternative would be

**Fig. 1.** Engineering a GPP-synthesizing microfactory in the yeast peroxisome. Conventional production of GPP-derived compounds in yeast relies on the endogenous cytosolic MVA pathway (shown in black). Here, we build an insulated pathway for GPP synthesis in the peroxisome by targeting the complete MVA pathway in the peroxisome (shown in green) and harvesting peroxisomal acetyl-CoA. Introduction of specific monoterpene synthases (*Se*CamS, *Sp*SabS, *Ob*GerS, *Ms*LimS, *Cl*LimS, *Pt*PinS, *Ob*GerS) in the peroxisome together with the GPP synthase Erg20p(N127W) (also shown in green) leads to strong increase in the production of the corresponding monoterpene scaffolds compared to the cytosol. When the monoterpene synthase and Erg20p(N127W) are targeted in the peroxisome in the absence of a peroxisomal MVA pathway, IPP and DMAPP coming from the cytosol (indicated by black arrows crossing the peroxisomal membrane) can still support synthesis of various monoterpenes, albeit at a lower level. Further oxidation of monoterpene scaffolds by cytochrome P450 enzymes (*Cr*G8OH and *Ms*LimH, also shown in green) residing at the ER provide precursors of high-value molecules, such as monoterpene indole alkaloids and menthol. The peroxisomal GPP pool can also be used for OA prenylation leading to CBGA, the common precursor of various cannabinoids. For further explanation of the steps and pathways, please refer to the legend embedded in the figure. HMG-CoA: 3-hydroxy-3-methylglutaryl-CoA A.

to establish GPP synthesis in a yeast organelle and cocompartmentalize the heterologous GPP-utilizing enzymes. Shielding GPP from a strongly competing pathway would allow a large enough GPP pool to build up and give the opportunity to enzymes with a lesser catalytic efficiency than Erg20p ($k_{cat}/K_M$ for GPP of $1.4 \times 10^5$ M$^{-1}$·s$^{-1}$) (14), such as monoterpene synthases ($k_{cat}/K_M$ in the range of $10^3$ to $10^4$ M$^{-1}$·s$^{-1}$) (10), to access the substrate.

To implement this strategy, we focused on the peroxisomes. In *S. cerevisiae*, the peroxisomes are a suitable target for organellar engineering because, in most culture conditions, they are not essential for cell viability (21) and their number and size can be modified in various ways to better fit the needs of the engineered pathway (22, 23). The yeast peroxisomes are the sites where β-oxidation of fatty acids takes place, creating a pool of acetyl-CoA that can be harvested by heterologous pathways, such as the

mevalonate (MVA) pathway that provides the isoprenoid precursors IPP and DMAPP (23, 24). Moreover, the peroxisomes have a single-layer membrane that allows a large number of low molecular weight compounds to travel across, either passively or through channel proteins, such as Pxmp2 (25). This can be advantageous for engineering the spatial confinement of substrates and enzymes, without restricting the exchange of precursors and products with the remaining of the cell or requiring the introduction of dedicated transporters (26). The peroxisomes are also detoxifying organelles that can handle and sequester more toxic molecules from the rest of the cell (27). Although other organelles, such as the mitochondria, could be used for a similar compartmentalization strategy, these are formed by double membranes, which can create a strong barrier to substrates or products, requiring considerable transport engineering for optimal performance. Furthermore, mitochondria carry out essential

functions for cell viability and, as such, cannot be extensively engineered without affecting yeast fitness (28). The above-mentioned favorable characteristics of the peroxisomes have led to their successful application in the production of medium-chain fatty alcohols, alkanes, olefins (23, 24), or alkaloids (29) in *S. cerevisiae*, penicillin in *Hansenula polymorpha* (30), poly-hydroxyalkanoates, and polylactic acid in *Pichia pastoris* and *Yarrowia lipolytica* (26, 31).

In this study, we demonstrate that the yeast peroxisomes can be advantageously repurposed for the production of GPP-derived molecules. We introduce a complete MVA pathway into the peroxisomes to establish efficient GPP-synthesizing microfactories that harvest the peroxisomal acetyl-CoA pool to produce a wide variety of GPP-derived compounds. We show that peroxisomal production can be used as a general strategy for the synthesis of monoterpene scaffolds by demonstrating that it results in important improvements in the production of several different compounds, including (*R*)-(+)-limonene, (*S*)-(-)-limonene, α-pinene, sabinene, camphene, and geraniol. Additionally, we show that the improved supply of monoterpene precursors, and likely the proximity of the peroxisomes to the endoplasmic reticulum (ER) (32–34), improve cytochrome P450-mediated oxidation of monoterpenes. This enables establishing the next step toward menthol and monoterpene indole alkaloid biosynthesis, through efficient production of *trans*-isopiperitenol and 8-hydroxygeraniol, respectively. The applicability of the peroxisome in the production of high-value molecules is exemplified even further by the synthesis of cannabigerolic acid (CBGA), the common precursor of cannabinoids. Finally, we evaluate this strategy in fed-batch fermentation and achieve titers of commercially important monoterpenes that bring them closer to industrial production without noticeable effects in strain fitness or viability. Our findings highlight peroxisomal engineering as an efficient strategy for the biotechnological production of high-value isoprenoids.

## Results

### Establishing Monoterpene Production in the Peroxisome.

To evaluate the suitability of the yeast peroxisomes for GPP-derived compound production, we set out to engineer monoterpene scaffold synthesis in the *S. cerevisiae* strain EGY48 (derivative of W303-A1) (*SI Appendix*, Table S1). We selected strain EGY48 because it does not harbor any prior genetic modification of the endogenous pathways involved in isoprenoid synthesis, allowing us to precisely investigate the impact of each intervention introduced in the process of establishing terpenoid biosynthesis in the different cellular compartments. As a target compound, we selected (*R*)-(+)-limonene, a highly valued fragrant compound (35) that is also used as a component of drop-in biofuels (36). To implement limonene synthesis, we employed *Cl*LimS, the (*R*)-(+)-limonene synthase from lemon (*Citrus limon*, *Cl*), which is a very efficient and highly specific enzyme (37) that produces only minute amounts of side-products beside (*R*)-(+)-limonene, whereas many monoterpene synthases are rather promiscuous enzymes producing multiple compounds (38).

Initially, *Cl*LimS was expressed from a high-copy plasmid vector and targeted to the cytosol of strain EGY48 (resulting in strain CYTLim01) (*SI Appendix*, Table S1). Under these conditions, a relatively low titer of 0.32 mg/L of (*R*)-(+)-limonene was obtained (Fig. 2*A* and *SI Appendix*, Table S2), in agreement with previous observations (10, 14, 39). When *Cl*LimS was directed to the peroxisome by the addition of a C-terminal SKL peroxisomal targeting signal-1 (PTS1; strain PERLim01) (*SI Appendix*, Table S1), a similar level of limonene production was observed (Fig. 2*A* and *SI Appendix*, Table S2). This suggested that *Cl*LimS was active in the peroxisome and that GPP could be translocated from the cytosol into the peroxisome, as it has previously been proposed to be the case for FPP (40, 41) or other metabolites (42).

In yeast, the isoprenoid precursors IPP and DMAPP are synthesized in the cytosol from acetyl-CoA through the MVA pathway. Fluxes through the MVA pathway are under tight feedback regulation from the membrane sterol and terpenol levels (43). Most metabolic engineering efforts to produce isoprenoids in yeast involve overexpression of the complete, or parts, of the
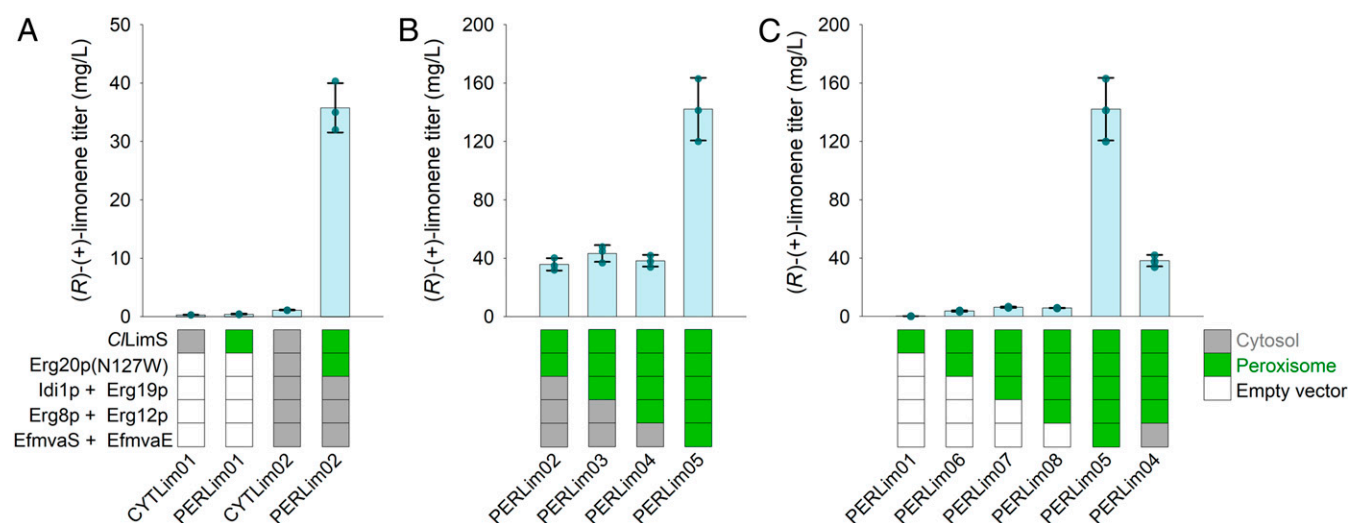
**Fig. 2.** Construction of a peroxisomal GPP-synthesizing pathway and its use for efficient production of (*R*)-(+)-limonene. (*A*) The (*R*)-(+)-limonene synthase *Cl*LimS was expressed in yeast cells and targeted to the cytosol (strain CYTLim01) or the peroxisome (strain PERLim01), respectively. Overexpression of the complete MVA pathway in the cytosol together with the GPP synthase Erg20p(N127W) only improved production by threefold (strain CYTLim02). However, switching the targeting of *Cl*LimS and Erg20p(N127W) to the peroxisome, under conditions where the MVA pathway in the cytosol is up-regulated (strain PERLim02), leads to a 32-fold increase in (*R*)-(+)-limonene production. (*B*) The heterologously expressed MVA pathway enzymes were sequentially shifted from the cytosol to the peroxisome enabling the utilization of the peroxisomal acetyl-CoA pool for efficient GPP production. An additional fourfold production increase was obtained upon construction of a full peroxisomal MVA pathway (PERLim05 vs. PERLim02). (*C*) Stepwise expression of the MVA and *R*-(+)-limonene pathway enzymes targeted to the peroxisome and their impact on (*R*)-(+)-limonene production in the absence of additional overexpression of the MVA pathway steps in the cytosol. Error bars correspond to the SD of the mean (*n* = 3, corresponding to three biological replicates).

MVA pathway (44). Thus, to improve (*R*)-(+)-limonene production, we overexpressed the entire MVA pathway in the cytosol from high copy-number plasmids. We used the *Enterococcus faecalis* EfmvaE and EfmvaS proteins to catalyze the first three steps of the pathway (corresponding to the steps catalyzed by the yeast Erg10p, Erg13p, and Hmg1/2p proteins) because of their high efficiency and the lack of feedback regulation of the *E. faecalis* MVA enzymes in yeast (39). For the subsequent steps, we used Erg8p, Erg12p, Erg19p, and Idi1p. Furthermore, we expressed the yeast FPP synthase variant Erg20p(N127W), which has been shown to function as an efficient GPP synthase (14). MVA pathway overexpression in the cytoplasm resulted in a 3.6-fold increase in (*R*)-(+)-limonene production to 1.13 mg/L (CYTLim02 vs. CYTLim01) (Fig. 2*A* and *SI Appendix*, Table S2). This is in accordance with previous observations that despite extensive engineering of the MVA pathway, production titers in the cytoplasm remain modest (10, 14, 39).

However, when, in the strain overexpressing the MVA pathway in the cytosol, only the GPP synthase Erg20p(N127W) and *Cl*LimS were shifted to the peroxisome (PERLim02) (*SI Appendix*, Table S1), (*R*)-(+)-limonene production improved drastically by 32-fold to reach 35.68 mg/L (Fig. 2*A* and *SI Appendix*, Table S2). This strong increase in limonene production confirms the initial hypothesis that the peroxisome is able to act as a barrier and insulate the locally formed GPP from the cytosolic Erg20p, allowing its efficient conversion by *Cl*LimS. Furthermore, it reveals that the precursors IPP and DMAPP can be efficiently transported to the peroxisome and be converted to GPP by Erg20p(N127W).

**Reconstructing a Full MVA Pathway in the Peroxisome.** To expand on these findings, we assessed the possibility to harvest the peroxisomal acetyl-CoA pool for GPP production in this organelle. To this end, we sequentially introduced the MVA pathway enzymes to the peroxisome, as it has been established that none of the MVA pathway enzymes is normally present in this organelle (45). Experiments were carried out both in cells with the upregulated MVA pathway in the cytosol (Fig. 2*B*) and in cells

without cytosolic MVA up-regulation (Fig. 2*C*), to separately evaluate the contribution of each step in the process. In the presence of Erg20p(N127W) and *Cl*LimS, sequential addition of Idi1p, Erg19p, Erg8p, and Erg12p in the peroxisome only had a minor impact on limonene production (PERLim03 and PERLim04 vs. PERLim02 in Fig. 2*B*; or PERLim07 and PERLim08 vs. PERLim06 in Fig. 2*C* and *SI Appendix*, Table S2). However, when the entire MVA pathway was assembled in the peroxisome (strain PERLim05) (*SI Appendix*, Table S1), a strong additional increase in limonene production, reaching 141 mg/L, was observed (Fig. 2 *B* and *C* and *SI Appendix*, Table S2; compare strain PERLim05 to strains PERLim02 or PERLim06). Thus, the heterologous peroxisomal MVA pathway is able to harvest the available pool of acetyl-CoA and direct it to monoterpene production. Moving the entire limonene-synthesizing pathway from the cytosol to the peroxisome gives an overall 125-fold improvement in production, compared to the titer of the strain expressing the same enzyme combination in the cytoplasm (PERLim05 vs. CYTLim02) (*SI Appendix*, Table S2). This dramatic increase clearly suggests that engineering a GPP-synthesizing microfactory in the peroxisome, taking advantage of the preexisting acetyl-CoA pool, can bypass current limitations in monoterpene production imposed by the strong competition of the sterol pathway in the yeast cytosol.

To avoid potential toxicity of the monoterpene products to the yeast cells when grown on solid media during strain manipulation (46), expression of the MVA pathway genes and the terpene synthase in these experiments is controlled using galactose-inducible promoters ($P_{GAL1}$ or $P_{GAL10}$). To confirm that the results obtained were not specific to using galactose as the carbon source, we evaluated monoterpene production using glucose-based growth media, which would be preferred for production in an industrial setting. To achieve this, the repressor *GAL80* gene was deleted in strain EGY48 (to give EGY48Δgal80) to allow Gal4p-mediated expression of the genes controlled by the $P_{GAL1}$ or $P_{GAL10}$ promoters in the absence of galactose. Subsequently, the entire cytosolic or peroxisomal pathway was introduced into EGY48Δgal80 to give strains CYTLim02Δgal80
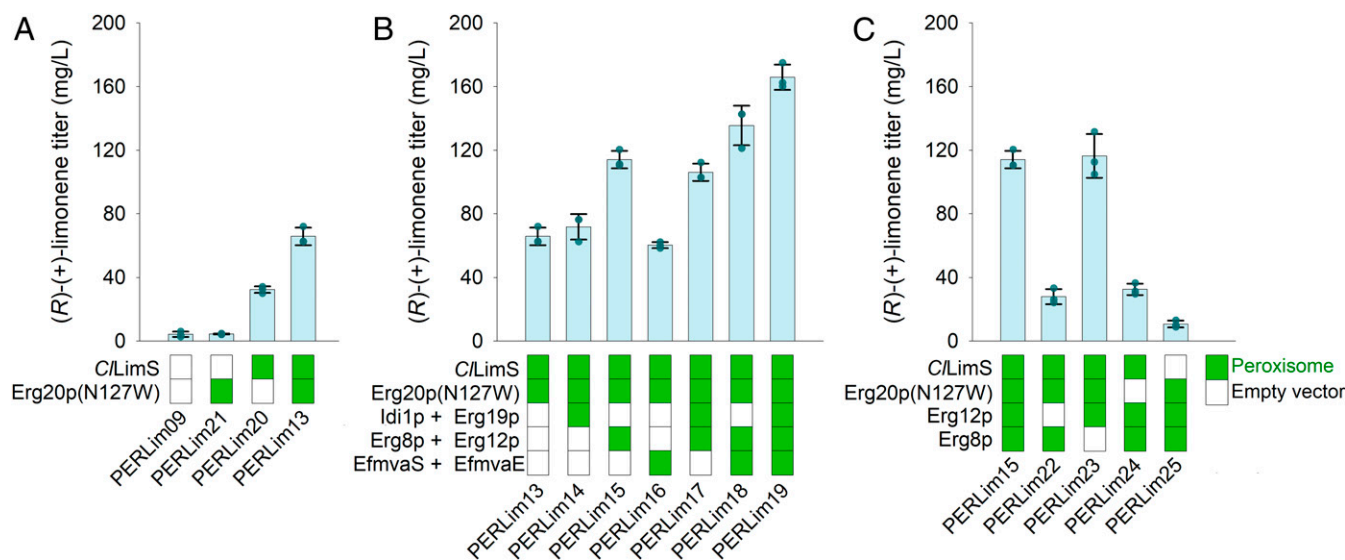


**Fig. 3.** Determining the limiting steps in the peroxisomal pathway. Combinatorial overexpression of the peroxisomal (*R*)-(+)-limonene pathway genes in strain PERLim09 to determine the limiting steps. (*A*) Strain PERLim09 was transformed with high copy-number episomal vectors overexpressing *Cl*LimS and/or Erg20p(N127W) (or the corresponding empty vector as control) and the effect of the up-regulation of the corresponding enzymes on (*R*)-(+)-limonene production was evaluated. (*B*) PERLim09 was transformed with high copy-number episomal vectors overexpressing the pathway genes in pairs (*IDI1* with *ERG19*, *ERG8* with *ERG12*, and *EfmvaS* with *EfmvaE*) under conditions where *Cl*LimS and Erg20p(N127W) were also overexpressed. (*C*) The contribution of individual overexpression of Erg12p and Erg8p was evaluated by transforming PERLim09 with high copy-number episomal vectors under conditions where *Cl*LimS and Erg20p(N127W) were also overexpressed. Error bars correspond to the SD of the mean (*n* = 3, corresponding to three biological replicates).

and PERLim05Δgal80, respectively. As shown in *SI Appendix,* *Fig. S1,* the (R)-(+)-limonene product titer achieved by strains CYTLim02Δgal80 and PERLim05Δgal80 in glucose-based media (1.66 mg/L and 131.2 mg/L, respectively) was very similar to the (R)-(+)-limonene titer achieved by strains CYTLim02 and PER-Lim05 in galactose-based media (1.13 mg/L and 141 mg/L, respectively). This confirms that the peroxisomal pathway is equally suited for the production of GPP-derived molecules using glucose as carbon source. We also evaluated the size and number of peroxisomes in the different sugar-based media using a PTS1-tagged form of GFP and found that the average number of peroxisomes in glucose-based media was 36% higher ($P = 0.000616$ determined by a paired $t$ test) than the average number in galactose/raffinose media (*SI Appendix,* *Fig. S2*). This could be advantageous for eventual glucose-based industrial production.

**Revealing Rate-Limiting Steps in the Peroxisomal GPP Pathway.** Despite the markedly improved production observed, the activity and stability of the enzymes targeted to the peroxisomes may still be compromised by the different physicochemical properties of this environment. Therefore, we proceeded to determine possible rate-limiting steps in the engineered peroxisomal pathway in order to identify targets for further optimization. To this end, a single copy of all of the genes of the MVA pathway (targeted to the peroxisome) together with the GPP synthase Erg20p(N127W) and *Cl*LimS was integrated into the genome of EGY48 to give the new chassis strain PERLim09. When strain PERLim09 was assessed for limonene production, a titer of 4.2 mg/L (Fig. 3*A* and *SI Appendix,* Table S3) was obtained, which was considerably lower than the strain expressing the same enzymes from episomal vectors (strain PERLim05) (*SI Appendix,* Table S2). This indicated that possible lower stability and activity of one or several of the enzymes of the pathway in the peroxisomal matrix requires high enzyme levels (high copy-number expression) for efficient production. To confirm this hypothesis and identify the limiting steps, each of the enzymes of the pathway were stepwise overexpressed via high copy-number episomal vectors in the base strain constructed above (PERLim09).

Initial up-regulation of *Cl*LimS and Erg20p(N127W) revealed that these two enzymes are main bottlenecks in the peroxisomal pathway, with their combined overexpression leading to a 16-fold increase in limonene production compared to the base strain (PERlim13 vs. PERLim09) (*SI Appendix,* Table S3). The more critical step appears to be that of the terpene synthase, as the limonene titer increased by eightfold by up-regulating only *Cl*LimS (PERLim20 vs. PERLim09) (Fig. 3*A* and *SI Appendix,* Table S3). Coupregulation of Erg20p(N127W) led to an additional twofold increase (PERLim13 vs. PERLim20), due to the improved availability of GPP (Fig. 3*A* and *SI Appendix,* Table S3). In contrast, the effect of Idi1p or Erg19p up-regulation was limited (Fig. 3*B* and *SI Appendix,* Table S3) (PERLim14 vs. PERLim13 and PERLim17 vs. PERLim15), suggesting that the corresponding enzymes do not catalyze a limiting step in this system. When the expression levels of Erg8p and Erg12p were up-regulated together, an additional twofold increase in limonene production was observed (Fig. 3*B* and *SI Appendix,* Table S3) (PERLim15 and PERLim17 vs. PERLim13). By investigating further the contribution of these two enzymes, we found that solely up-regulating Erg12p in strain PERLim23 was sufficient to afford the high titers seen in strain PERLim15, while increased Erg8p levels barely affected limonene production (PERLim22) (Fig. 3*C* and *SI Appendix,* Table S3). Finally, EfmvaE/S up-regulation induced a 30% further increase in production (PERLim19), but only when the previous bottlenecks in the pathway were already resolved: That is, when combined with *Cl*LimS, Erg20p(N127W) and Erg12p up-regulation, as highlighted by the similar (R)-(+)-limonene production of strain

PERLim16 compared to PERLim13 (Fig. 3*B* and *SI Appendix,* Table S3).

These results suggest that, for the most part, the reconstituted MVA pathway functions efficiently in the peroxisome. The most crucial step in the peroxisomal MVA pathway is that of Erg12p, requiring high-level expression for optimal function, while Erg8p, Idi1p, Erg19p, and EfmvaE/S play a less critical role and lower level expression is sufficient to support a high flux. On the other hand, the terpene synthase (*Cl*LimS), and to a lesser extend the GPP synthase [Erg20p(N127W)], appear to be the main bottlenecks in terpene production. This indicates that the MVA pathway provides adequate amounts of IPP and DMAPP precursors, which, in turn, require high-level expression of the GPP synthase and the terpene synthase to be fully harvested. Thus, further efforts toward improving peroxisomal monoterpenoid production could focus on optimizing, primarily, the terpene synthase and GPP synthase steps and, secondarily, the MVA kinase Erg12p.

**Peroxisomal Production as a General Strategy for Monoterpenes.** To assess whether the peroxisomal strategy was applicable to monoterpene production in general, and not only for (R)-(+)-limonene, we evaluated additional monoterpene synthases, displaying a range of product specificity and enzymatic efficiency. We selected camphene synthase from *Solanum elaeagnifolium* (*Se*CamS), α-pinene synthase from *Pinus taeda* (*Pt*PinS), sabinene synthase from *Salvia pomifera* (*Sp*SabS), and (S)-(-)-limonene synthase from *Mentha spicata* (*Ms*LimS), and compared synthesis of their main product in the cytosol and the peroxisome. The same positive effect of peroxisome targeting was observed with an improvement of 15-, 22-, 17-, and 105-fold for camphene (PER-Cam02 vs. CYTCam02), sabinene (PERSab02 vs. CYTSab02), (S)-(-)-limonene (PERLim27 vs. CYTLim04), and α-pinene (PERPin02 vs. CYTPin02), respectively, compared to cytosolic production by the same enzymes (Fig. 4 and *SI Appendix,* Table S4). The differences in the extent of improvement in monoterpene production observed between the five enzymes tested (including *Cl*LimS) likely reflect the different efficiency or stability of each monoterpene synthase. Indeed, as shown in the previous section (Fig. 3), the production level of the engineered peroxisomal pathway is primarily dictated by the capacity of the terpene synthase. Overall, the systematic significant increase in monoterpene production for all products tested further confirms the applicability of peroxisomal engineering as a general and powerful strategy for the production of GPP-derived molecules.

**Peroxisomal Production Facilitates Downstream Oxidation Steps.** Many valuable monoterpenoids are synthesized by further modification of the basic monoterpene scaffold produced by the terpene synthases. Such downstream events frequently involve site-specific oxidation by cytochrome P450 enzymes. However, production of oxygenated monoterpenes in yeast has so far been very inefficient (10). This has been attributed to the poor production of the terpene scaffold and, potentially, the difficulty in directing a sufficient fraction of cytosolically produced monoterpene hydrocarbons to the ER-localized cytochrome P450s. Having obtained significant improvements in monoterpene scaffold production using the peroxisomal pathway, and considering the proximity of the peroxisome to the ER, we evaluated the applicability of the peroxisomal strategy in the synthesis of hydroxylated high-value products. To this end, we set out to establish production of *trans*-isopiperitenol, the first oxidation step toward the synthesis of (-)-menthol (Fig. 1). Menthol is the second-most used flavor and fragrance in confectionery products and personal hygiene goods (47) and is widely used in nonprescription medicines as topical analgesic or decongestant (47). Since the biosynthesis of (-)-menthol is based on the (S)-(-) stereoisomer of limonene, we sought to capitalize on the
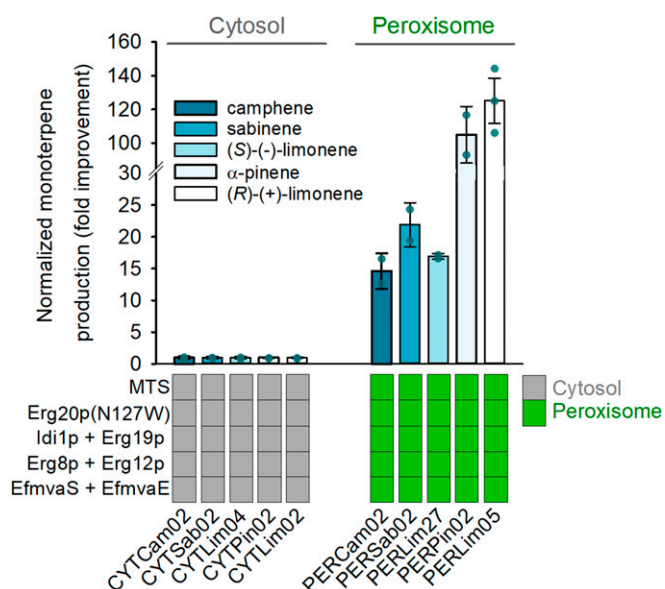
**Fig. 4.** Peroxisomal compartmentalization is a general strategy for monoterpene production in yeast. Four different monoterpene synthases (MTS) (*Se*CamS, *Sp*SabS, *Ms*LimS, and *Pt*PinS) were expressed in cells producing GPP from the up-regulated cytosol-based MVA pathway (left side) or the engineered peroxisomal pathway (right side). To facilitate comparison, production titers for each monoterpene compound were normalized to the titer of the strain expressing the corresponding synthase and the MVA pathway in the cytoplasm. Error bars correspond to the SD of the mean (*n* = 2, corresponding to two biological replicates).

significant production improvement of this molecule in the peroxisome (Fig. 4) by engineering a yeast strain harboring the peroxisomal GPP pathway together with the (*S*)-(-)-limonene synthase *Ms*LimS and the limonene-3-hydroxylase/*trans*-isopiperitenol synthase *Ms*LimH from *M. spicata*. The cytochrome P450 reductase *Tc*CPR from *Taxus cuspidata* was also introduced to facilitate electron transfer to *Ms*LimH, giving rise to strain PERLim30. Furthermore, a version of strain PERLim30 harboring an empty vector instead of the *Ms*LimH and *Tc*CPR encoding genes was constructed as a control strain (PERLim29).

For comparison, we also established a strain producing *trans*-isopiperitenol based on cytosolic (*S*)-(-)-limonene synthesis (CYTLim06) by introducing *Ms*LimS, *Ms*LimH, and *Tc*CPR in the strain overexpressing the cytosolic MVA pathway. Following gas chromatography (GC)-MS and GC-flame ionization detection (FID) analysis, we obtained production of *trans*-isopiperitenol in both the cytosolic and the peroxisomal (*S*)-(-)-limonene producing strains (Fig. 5*A*). *Trans*-isopiperitenol was the main oxidation product and only minor side-products were observed, likely corresponding to regioisomers of *trans*-isopiperitenol, as reported previously for *Ms*LimH (48). However, while the *trans*-isopiperitenol titer in CYTLim06 was only 0.28 mg/L, the titer of peroxisome-based *trans*-isopiperitenol production in PERLim30 was 69-times higher, reaching 19.24 mg/L (Fig. 5*A*). Notably, whereas the conversion of (*S*)-(-)-limonene to *trans*-isopiperitenol in the strain producing the precursor in the cytosol (CYTLim06) was 14%, the overall oxidation efficiency in the peroxisome-based system was 2.5 times higher, achieving conversion of 37% of (*S*)-(-)-limonene into *trans*-isopiperitenol. The observation that the efficiency of conversion increases in the case of the peroxisomal platform cannot be explained solely by the improved production of substrate and indicates that there may be additional factors that contribute to

the increase, such as the availability of the substrate to the P450 system.

**Production of a Monoterpene Indole Alkaloid Precursor.** In addition to monoterpenoids, GPP also serves as a building block for the synthesis of numerous other compounds that contain a C10 isoprenoid moiety. Characteristic examples are the iridoids and monoterpene indole alkaloids. The latter include vinblastine and vincristine, two anticancer agents with broad use in clinical practice (8, 9, 12). The early steps in the biosynthetic pathway leading from GPP to iridoids and monoterpene indole alkaloids involve the synthesis of the monoterpene alcohol geraniol and its subsequent conversion to 8-hydroxygeraniol (Fig. 1). Therefore, we set out to evaluate the contribution of the peroxisomal pathway in the production of 8-hydroxygeraniol. Initially, we established efficient geraniol production in the peroxisome by introducing *Ocimum basilicum* geraniol synthase (*Ob*GerS) into a strain engineered for peroxisomal GPP production, to obtain PERGer02, producing 288.65 mg/L geraniol. Subsequently, we introduced the geraniol 8-hydroxylase from *Catharanthus roseus* (*Cr*G8OH; CYP76B6) into strain PERGer02, together with the cytochrome P450 reductase (*Cr*CPR) from the same species to give strain PERGer04 (or an empty vector carrying the *LEU2* marker to give PERGer03 control strain). As shown in Fig. 5*B*, strain PERGer04 was able to convert geraniol to 8-hydroxygeraniol, whereas strain PERGer03, lacking the geraniol 8-hydroxylase and the cytochrome P450 reductase, was only able to produce geraniol. An overall titer of 25.11 mg/L 8-hydroxygeraniol in shake flask batch cultivation was obtained, establishing an alternative solution for a challenging step in the reconstruction of the monoterpene alkaloid pathway in yeast (8).

**Production of CBGA in the Peroxisome.** We evaluated the applicability of the peroxisomal GPP-synthesizing microfactory in the production of another group of GPP-derived high-value compounds, that of cannabinoids. In the cannabinoid biosynthetic pathway, olivetolic acid (OA) is prenylated by GPP to form CBGA via the action of a dedicated geranyl transferase (Fig. 1). CBGA is a key compound in the pathway because it is the precursor of different cannabinoids, such as tetrahydrocannabinolic acid (THCA) and cannabidiolic acid (CBDA). In yeast, low GPP availability in the cytosol can create a bottleneck in the process of producing high titers of cannabinoids. Here, the GPP synthase Erg20p(N127W) and the geranyldiphosphate:olivetolate geranyltransferase from *Cannabis sativa*, *Cs*PT4 (11), were targeted to the yeast peroxisome for CBGA production. Both genes were introduced into strain EGY48 under the control of the inducible promoters P*GAL1* and P*GAL10*, to give strain PERCan01, and together with the MVA pathway genes, to give strain PERCan02. A strain expressing the peroxisomal MVA pathway enzymes without Erg20p(N127W) and *Cs*PT4 was constructed as a negative control and named PERMva01. Following growth in complete minimal media under galactose-induced conditions and supplementation with OA (0.5 mM), production of CBGA was analyzed by LC-MS. As shown in Fig. 6, strain PERCan02 was able to geranylate OA to form CBGA, while strain PERMva01, lacking Erg20p(N127W) and *Cs*PT4, and strain PERCan01, lacking a functional GPP-synthesizing pathway in the peroxisome, were unable to convert OA. Overall, we obtained 0.82 mg/L CBGA. These results demonstrate that *Cs*PT4 is active in the peroxisome and OA can be transported or diffuse into the organelle, supporting efficient OA geranylation. Complete biosynthesis of CBGA from sugar requires the introduction of six additional steps, responsible for the conversion of acetyl-CoA to OA. Reconstruction of the OA-synthesizing branch of the cannabinoid pathway into the peroxisome will enable the complete peroxisomal production of CBGA.
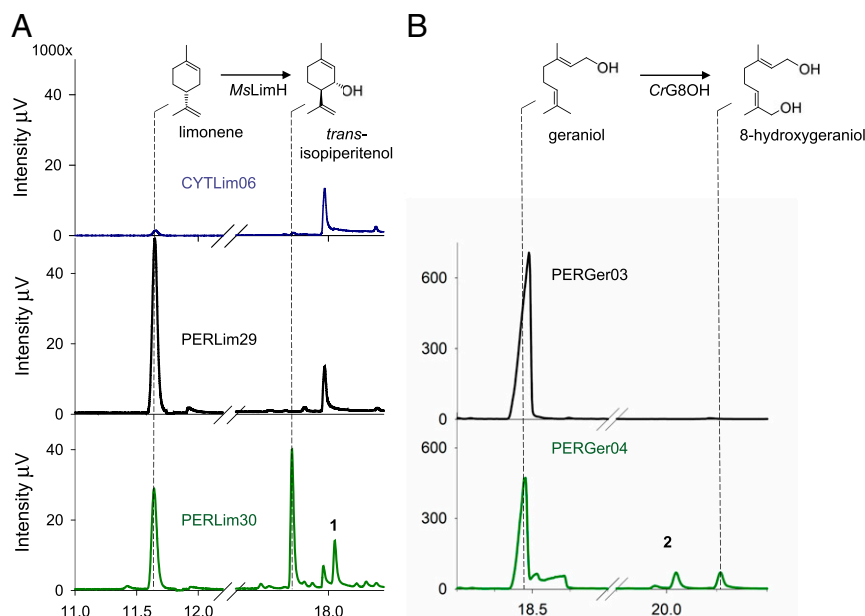
**Fig. 5.** Peroxisomal production facilitates cytochrome P450-mediated hydroxylation of (*S*)-(-)-limonene and geraniol. (*A*) Production of *trans*-isopiperitenol. Metabolites extracted from batch cultures of strains PERLim29 (negative control), PERLim30 [expressing *Ms*LimH and *Tc*CPR in the peroxisomal (*S*)-(-)-limonene production background] and CYTLim06 [expressing *Ms*LimH and *Tc*CPR in the cytosolic (*S*)-(-)-limonene production background] were analyzed by GC-FID and the chromatograms are shown in black, green, and blue, respectively. (*B*) Production of 8-hydroxygeraniol. Metabolites extracted from batch cultures of strains PERGer03 (control strain producing geraniol in the peroxisome) and PERGer04 (strain producing geraniol in the peroxisome and expressing the geraniol hydroxylase and the corresponding P450 reductase) were analyzed by GC-FID and the chromatograms are shown in black and green, respectively. Mass spectra information of the *trans*-isopiperitenol peak and peak 1 in strain PerLim30 and the 8-hydroxygeraniol peak in strain PerGer04 are reported in *SI Appendix*, Figs. S3 and S4.

**High Titers of Key Monoterpenes by Fed-Batch Cultivation.** Because of the industrial significance of several GPP-derived molecules, we evaluated the performance of the developed peroxisomal pathway in fed-batch cultivation. We focused on two compounds due to their commercial importance. Geraniol is one of the most widely used molecules in the flavor and fragrance sector and a common ingredient in consumer products (49), with a production that exceeds 1,000 t per annum (50). The second compound selected was (*R*)-(+)-limonene, because of its wide application as a fragrance in consumer products (49), but also as precursor for various biomaterials (35) and drop-in biofuel (36).

Semicontinuous fed-batch experiments with strains PERGer02 for geraniol production and PERLim19, for (*R*)-(+)-limonene production, resulted in a continuous accumulation of monoterpene products that was proportional to the amount of biomass formed (Fig. 7). Final titers of 5.52 g/L of geraniol (Fig. 7*A*) and 2.58 g/L of (*R*)-(+)-limonene (Fig. 7*B*) were obtained. We attribute the fact that the geraniol titer was higher than the (*R*)-(+)-limonene titer to the different efficiency of the corresponding terpene synthase. Examination of the published kinetic data for these two enzymes revealed that the catalytic efficiency $k_{cat}/K_M$ for *Ob*GerS is $3.8 \times 10^4$ M$^{-1}$·s$^{-1}$, while for *Cl*LimS it is $1.2 \times 10^4$ M$^{-1}$·s$^{-1}$ (10, 51). We found no evidence for product toxicity by geraniol or (*R*)-(+)-limonene under conditions mimicking various levels of end-product accumulation, which we attribute to the efficiency of the isopropyl myristate overlay to trap the monoterpenes produced (*SI Appendix*, Fig. S5). Notably, we observed no difference in the growth of yeast cells harboring the peroxisomal pathway compared to the cells harboring the pathway in the cytosol (*SI Appendix*, Fig. S6), suggesting that the engineered strains are robust, even at the demanding conditions of high-density fermentation, establishing a solid base for further peroxisomal engineering and additional production improvements.

## Discussion

Engineering of microorganisms for the production of valuable molecules is a sustainable alternative to conventional production methods, already providing a solution for the production of numerous compounds amounting to a $230 billion global market (52). However, achieving economically viable titers and productivity is still a major roadblock in the process of reaching industrial production of several valuable compounds. In this effort, obstacles often arise from the undesirable cross-talk between heterologous and native pathways that is rooted in the use of common intermediates and the structural similarity between metabolites (4). To overcome these challenges, herein we converted the yeast peroxisome into a dedicated compartment for the production of monoterpenes and other GPP-derived high-value compounds. Our approach has strong similarities with the strategy used by plant cells to produce GPP-derived compounds. In plants, monoterpene synthesis takes place in the chloroplast, using precursors provided by the chloroplast-based MEP pathway that converts pyruvate and glyceraldehyde-3-phosphate to IPP and DMAPP. In this way, GPP-dependent synthesis of monoterpenes, and GGPP-dependent biosynthesis of diterpenes, chlorophyll, and carotenoids are insulated in the chloroplast from the competing FPP-utilizing sterol biosynthesis pathway that takes place in the plant cytosol. As an analogy to the plant chloroplast, we introduce into the yeast peroxisome a complete MVA pathway to synthesize GPP from acetyl-CoA.

Using peroxisomal production, we achieve monoterpene production titers that were not previously possible and provide a unique example of how the yeast peroxisome can be converted into a dedicated organelle for efficient bioproduction, something that has so far been possible only for the synthesis of fatty alcohols (23, 24). Although the peroxisome has previously been utilized for the production of two other isoprenoids, the sterol
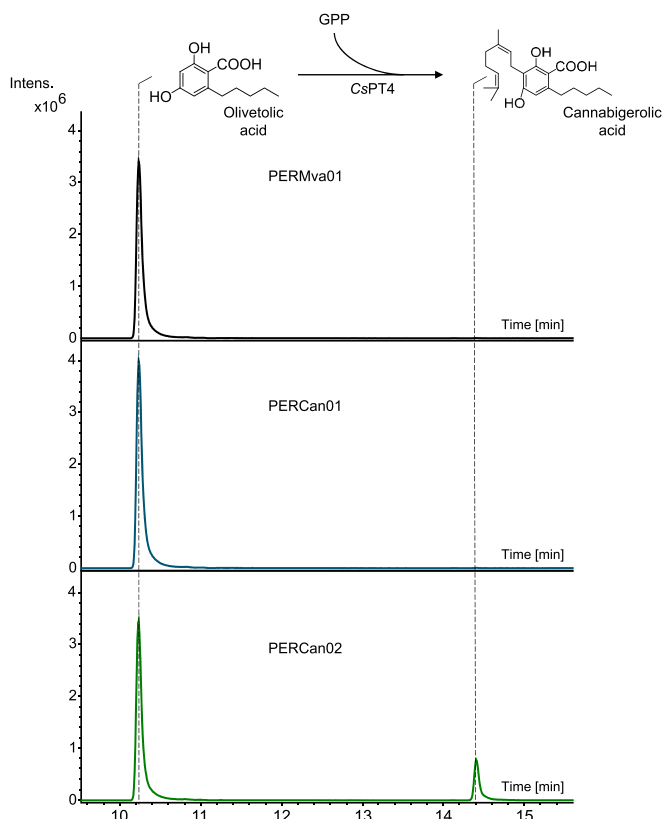
**Fig. 6.** Use of the peroxisomal GPP-synthesizing microfactory for the production of CBGA. The geranyl transferase *CsPT4* from *C. sativa* and the GPP synthase Erg20p(N127W) from *S. cerevisiae* were introduced into yeast cells producing GPP from the engineered peroxisomal pathway, to give strain PERCan02. Conversion of OA into CBGA is observed in strain PERCan02 compared to the control strains lacking *CsPT4* and Erg20p(N127W) (strain PERMva01) or lacking the peroxisomal GPP-producing pathway (strain PER-Can01). OA and CBGA presence in the extracts was assessed by LC–electrospray ionization–MS analysis and extracted ion chromatograms for the mass of OA (223.0982 ± 0.02 g/mol) and CBGA (359.2226 ± 0.02 g/mol) are presented here.

precursor squalene and the sesquiterpene α-humulene, the peroxisomal pathway alone could not outperform cytosolic production (53) and at best equaled it (41). However, in the case of squalene and α-humulene, a similar beneficial effect of establishing a peroxisomal pathway, as we observed for monoterpenes, would not be anticipated. Both these compounds are synthesized

from FPP, and yeast cytosolic metabolism is already optimized for the synthesis of FPP as an integral part of sterol biosynthesis.

In the approach presented here, monoterpene production in the peroxisome reached an overall 15- to 125-fold increase over cytosolic production for all monoterpene compounds tested. Cultivation of the developed strains in semicontinuous fed-batch conditions led to the production of 5.5 g/L geraniol and 2.6 g/L (*R*)-(+)-limonene. Although we used a basic system, without extensive genetic or protein engineering, in order to facilitate comparison between cytosolic and peroxisomal production, the product titers obtained compare favorably to other yeast-produced monoterpene titers reported to date (10, 19, 20, 54). For example, Cheng et al. (19). obtained 0.9 g/L (*R*)-(+)-limonene using both GPP-based and neryl diphosphate-based production in combination with dynamic control at the Erg20p node. However, when only the GPP-based pathway was used (as is the case in our experiments), the (*R*)-(+)-limonene titer was considerably lower, at 0.14 g/L. Moreover, Jiang et al. (20) obtained 1.68 g/L geraniol following extensive protein engineering of the geraniol synthase. Using this engineered terpene synthase variant could help improve geraniol production in the peroxisome even further. Significant additional yield improvements in peroxisomal production can be obtained by introducing the many genetic and metabolic engineering interventions already established to facilitate isoprenoid production in yeast (1, 55), including improving cofactor availability (18), redox and pathway balancing (2), dynamic transcriptional control (10), improvement of protein stability and activity (56), strain fitness (57), and so forth.

*S. cerevisiae* is a preferred host for the industrial production of high-value isoprenoids because it can support functional expression of cytochrome P450 enzymes involved in scaffold decoration (58). We utilized the peroxisome-engineered strains for P450-driven hydroxylation of (*S*)-(-)-limonene into *trans*-isopiperitenol and established an example of bio-production of this menthol intermediate in yeast. Production of natural menthol from plant extracts requires expensive downstream processes, such as filtration and steam-distillation, and can hardly meet market demand. This has led to increased use of synthetic menthol from petrochemical sources, accounting to 30% of the global production (47), which is, in turn, prompting for its sustainable production using microorganisms. Establishment of efficient *trans*-isopiperitenol production will pave the way to reconstruct the full pathway and eventually achieve biotechnological production of menthol.

We found that, using the peroxisomal pathway, the efficiency of hydroxylation was markedly improved compared to previous efforts (10), reaching 37% conversion of (*S*)-(-)-limonene into *trans*-isopiperitenol. We hypothesize that peroxisomal production of
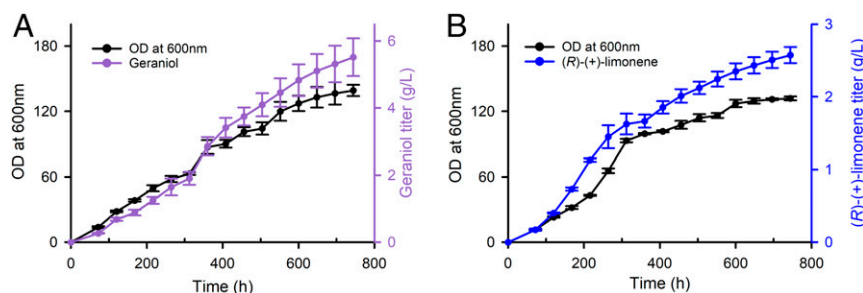


**Fig. 7.** Fed-batch culture production of geraniol and (*R*)-(+)-limonene by harnessing the engineered peroxisomal monoterpene pathway. Semicontinuous fed batch flask cultures of strains PERGer02 and PERLim19 were conducted to evaluate the maximal monoterpene production of the peroxisomal pathway under high cell-density conditions. In both cases, cultures could be sustained over a prolonged period of time allowing for a continuous and steady production of the corresponding monoterpene. (*A*) Cell optical density and geraniol production by strain PERGer02. (*B*) Cell optical density and limonene production by strain PERLim19. Cultures were fed with galactose/raffinose and the pH adjusted back to 4.5 every 48 h. Error bars correspond to the SD around the mean (*n* = 3, corresponding to three biological replicates).

monoterpenes greatly enhances downstream hydroxylation steps because of the increased substrate concentration and the proximity of the peroxisome membrane to the ER, where the cytochrome P450 enzymes normally reside (34, 59). The biogenesis of the peroxisome is based on the redistribution of membrane lipids and proteins from the ER and a dynamic exchange of these building blocks between the two has been well-documented (32, 33, 60). This communication is supported by the physical association of the peroxisomes with the ER, mediated by characterized tethering proteins (34, 61). The physical contact of these organelles can facilitate the transport of the lipophilic terpene scaffolds from the peroxisome, where they are produced, to the ER, where they undergo cytochrome P450 oxidation, by solubilization and movement within the membranes. Moreover, the similar composition of the ER and peroxisomal membranes and the frequent exchange of proteins between them implies that the peroxisome membrane may also harbor heterologously expressed cytochrome P450 enzymes, particularly under conditions of protein overexpression. Thus, producing the terpene scaffolds in the peroxisome provides an effective strategy for the production of oxygenated products and further engineering of cytochrome P450-mediated oxidation focusing on this organelle may lead to additional conversion improvements.

In addition to monoterpenoids, there are many other high-value compounds that contain a GPP-derived moiety. Well-studied examples include various alkaloids, such as the monoterpene indole alkaloids, and prenylated aromatic compounds, like the cannabinoids. The peroxisomal GPP pathway established here can have additional applications in the production of these bioactive meroterpenoid compounds, which constitute a rapidly expanding market. Here, we establish proof of concept for the synthesis of these molecules using the peroxisomes by achieving production of 8-hydroxygeraniol and CBGA, key starting compounds in each pathway, respectively. Further engineering of the subsequent steps of these GPP-dependent pathways could establish efficient platforms for the production of valuable compounds.

We observed a strong capacity of the developed strains to maintain a steady production over a prolonged period of time without any notable impact on growth and survival. This indicates that peroxisome engineering for monoterpene production does not introduce a pronounced burden on cellular function or decrease strain fitness. Previous research on subcellular compartmentalization of monoterpene production in the mitochondria resulted in strong decrease in growth and cell viability (28), suggesting that the essential nature of the mitochondria limits the extent by which they can be engineered without compromising the integrity of metabolism. Thus, the robustness of production in our system confirms the potential of the peroxisome as a powerful tool for metabolic engineering. Further modification of the number and size of peroxisomes, as reported in related studies (5, 23, 24), could yield additional production improvements without compromising cellular fitness. Notably, increasing peroxisome proliferation, by a combined strategy of deletion and overexpression of several *PEX* genes, have proven to be an effective strategy to improve production of heterologous compounds by circumventing the limited peroxisome population found in *S. cerevisiae* under standard growth conditions (23). Additionally, the productivity of the peroxisomal microfactory could be further increased by engineering fatty-acids accumulation and degradation (62) and thus providing a more substantial supply of acetyl-CoA in this organelle.

At the conceptual level, here we develop yeast organelles as synthetic biology devices. These devices can be exploited for the modular assembly and optimization of complex pathways, allowing efficient troubleshooting and fine-tuning, while maintaining orthogonality. This approach adds an extra level of hierarchical abstraction in the systematic engineering of cell factories.

## Methods

**Chemicals and Enzymes, Yeast Media, Growth Conditions, Transformation Procedures, and Analytical Procedures.** Detailed methods can be found in *SI Appendix*.

**Gene Cloning in *Escherichia coli* and Yeast Expression Vectors.** All of the plasmid constructions (*SI Appendix*, Tables S5 and S6) were made using the *E. coli* Mach1 strain (Thermo Fisher Scientific). *SI Appendix*, Table S7 contains all primers used in cloning procedures described below. Four uracil-specific excision-reagent (USER) vectors with uracil, tryptophan, leucine, or histidine as auxotrophic markers were used for episomal gene expression. pESC-URA-USER (pCfB132), pESC-LEU-USER (pCfB220), and pESC-HIS-USER (pCfB291) were gift from Prof. Irina Borodina (Technical University of Denmark, Kongens Lyngby, Denmark) and pESC-TRP-USER (pWUS) was constructed by replacement of the *URA3* gene with *TRP1* on pCfB132. All genes used in this study that are from yeast origin were directly amplified from EGY48 genomic DNA. Yeast codon-optimized versions of *C. limon* (R)-(+)-limonene synthase (*Cl*LimS; GenBank AF514287.1), *M. spicata* (S)-(-)-limonene synthase (*Ms*LimS; GenBank Q6IV13), *P. taeda* α-pinene synthase (*Pt*PinS; GenBank Q84KL3.1), *S. pomifera* sabinene synthase (*Sp*SabS) (63) (GenBank A6XH06), *S. elaeagnifolium* camphene synthase (*Se*CamS) (64), and *O. basilicum* geraniol synthase (*Ob*GerS; GenBank Q6USK1.1) were obtained by gene synthesis (GeneArt, Thermo Fisher Scientific) (*SI Appendix*, Table S8). In addition, the synthetic fragments bear flanking regions containing specific restriction sites and a generic sequence compatible for USER cloning. The above genes were amplified and cloned by USER cloning into the yeast expression vectors using primers "GeneName"-FP and "GeneName"-RP or "GeneName"-SKL-RP to introduce compatible USER overhangs with the corresponding promoter part (*SI Appendix*, Table S7) and the digested AsiSI/*Nb.*BsmI USER cassette of the pESC-URA/LEU/HIS/TRP-USER backbone. By applying the USER cloning technique (65), one or two genes of interest and a uni- or bidirectional promoter of choice were simultaneously integrated into the backbone vectors by specific annealing of the overhang created between the PCR parts and digested USER cassette (66). Peroxisomal targeting of proteins was ensured by C-terminal addition of the tripeptide SKL utilizing the following nucleotide sequence 5′-TCCAAGCTG-3′ while removing the original stop codon and replacing it with 5′-TAA-3′.

**Construction of Yeast Integration Vectors.** Yeast integrative vectors (*SI Appendix*, Table S6) were constructed in *E. coli* Mach1 strain (Thermo Fisher Scientific). *SI Appendix*, Table S7 contains all primers used in cloning procedures described below. Five integrative vectors (pAS1_X-3- pAS3_X-3) (*SI Appendix*, Tabl+e S6) were used to insert genes of interest at a well-characterized site in the *S. cerevisiae* genome. Integration of genes of interest were targeted to site 3 on chromosome X, a region known for high gene expression with low to no impact on growth rate (67). Empty integration vectors were kindly provided by Victor Forman, University of Copenhagen, Denmark, with modifications to the system described by Vanegas et al. (68) to enable insertion of up to 10 genes at one locus. Genes and promoters were amplified utilizing primers containing USER-compatible overhangs; see *SI Appendix*, Table S7 for primers. PCR fragments were USER cloned into AsiSI/*Nb.*BsmI digested empty vectors to assemble promoter, gene, and terminator parts. Combinations of genes, promoters, and terminators can be seen in *SI Appendix*, Table S6. pAS1_X-3 contains an ampicillin-resistance gene (AmpR), a *Kluyveromyces lactis* URA3 gene and a region homologous to the insertion site, X3-DOWN, and a homologous region to pAS2A. To this vector *Efm*vaS-SKL and *Efm*vaE-SKL were assembled with a bidirectional $P_{GAL1}$-$P_{GAL10}$ promoter and tPGI1/CYC1 terminators, respectively, to give pIntPER01. pAS2A contained AmpR, homologous regions to pAS1_X-3 and pAS2B and were assembled with a bidirectional $P_{TDH3}$-$P_{SED1}$ promoter, *ERG8*-SKL and *ERG12*-SKL, and tPRM8/tFBA1 terminators to give pIntPER02. pAS2B contained AmpR, homologous regions to pAS2A and pAS2C, and was assembled with a single $P_{FBA1}$ promoter, *ERG19*-SKL, and tSPG5 terminator to give pIntPER03. pAS2C contained AmpR, homologous regions to pAS2B and pAS3_X-3 and was assembled with a single $P_{CCW12}$ promoter, *IDI1*-SKL and tENO2 terminator to give pIntPER04. pAS3_X-3 contained AmpR, homologous regions to pAS2C and the genomic insertion site, X3-UP. pAS3_X-3 was assembled with a bidirectional $P_{PGK1}$-$P_{TEF1}$ promoter, *Cl*LimS-SKL and *ERG20*(N127W)-SKL and tTDH2/tADH1 terminators to give pIntPER05, with *Ob*GerS-SKL and *ERG20*(N127W)-SKL to give pIntPER06 or with *Ms*LimS-SKL and *ERG20*(N127W)-SKL to give pIntPER07. Prior to yeast transformation integrative vectors were digested with NotI according to manufacturer's protocol. Removal of the *Kl*URA3 marker, which was flanked by direct repeat sequences, was achieved by utilizing

plates containing 5-fluoroorotic acid. Genotyping was performed by PCR and subsequent sequencing.

**Bacterial Strains and Plasmids.** All bacterial strains, yeast strains, and plasmids used or derived from this study are listed in *SI Appendix*, Tables S1, S5, and S6. Strain EGY48Δgal80 was constructed by amplifying the *GAL80* deletion cassette from the plasmid pAS_Δgal80 with the GAL80-UP-FP and GAL80-DOWN-RP and transforming EGY48 with the resulting PCR product. Strain PERLim09 was constructed by insertion of one copy of all of the genes encoding for the peroxisomally targeted MVA pathway enzymes (EfmvaS, EfmvaE, Erg8p, Erg12p, Erg19p, and Idi1p) together with Erg20p(N127W) and *Cl*LimS into the genome of EGY48 on chromosome X using the integration vectors pIntPER1-5. Strains PERLim28 and PERGer01 were constructed following the same approach but by replacing *Cl*LimS (pIntPER5) by *Ms*LimS (pIntPER6) or *Ob*GerS (pIntPER7), respectively. Strain PERLim30 was derived from PERLim28, by subsequent introduction of the limonene-3-hydroxylase from *M. spicata* (*Ms*LimH/CYP71D95) and the cytochrome P450 reductase *Tc*CPR from *T. cuspidata*, together with additional copies of the rate-limiting enzymes of the pathway, using high copy-number episomal vectors, as determined with the study of the (*R*)-(+)-limonene production pathway. In a similar way, strain PERGer04 was obtained from PERGer01 by the introduction of the 8-hydroxygeraniol synthase from *C. roseus* (*Cr*G8OH) and the cytochrome P450 reductase *Cr*CPR from the same species.

**Data Availability.** All study data are included in the article and supporting information.

1. J. Nielsen, J. D. Keasling, Engineering cellular metabolism. *Cell* **164**, 1185–1197 (2016).
2. P. K. Ajikumar *et al.*, Isoprenoid pathway optimization for Taxol precursor overproduction in Escherichia coli. *Science* **330**, 70–74 (2010).
3. V. J. J. Martin, D. J. Pitera, S. T. Withers, J. D. Newman, J. D. Keasling, Engineering a mevalonate pathway in Escherichia coli for production of terpenoids. *Nat. Biotechnol.* **21**, 796–802 (2003).
4. M. T. Alam *et al.*, The self-inhibitory nature of metabolic networks and its alleviation through compartmentalization. *Nat. Commun.* **8**, 16018 (2017).
5. S. K. Hammer, J. L. Avalos, Harnessing yeast organelles for metabolic engineering. *Nat. Chem. Biol.* **13**, 823–832 (2017).
6. Essential Oils Market, Essential oils market size by product type (orange, lemon, lime, peppermint, citronella, jasmine), method of extraction, application (food and beverage, cosmetics and toiletries, aromatherapy, home care, health care), and by region—Global report, 2017–2022, https://www.marketsandmarkets.com/Market-Reports/essential-oil-market-119674487.html#:~:text=%5B176%20Pages%20Report%5D%20The%20global,major%20factors%20driving%20the%20market. Accessed 21 October 2020.
7. FinancialNewsMedia.com, Global medical cannabinoid market expected to reach $44 Billion by 2024, https://www.prnewswire.com/news-releases/global-medical-cannabinoid-market-expected-to-reach-44-billion-by-2024-300929410.html#:~:text=2%2C%202019%20%2FPRNewswire%2F%20%2D%2D,by%202024%2C%20according%20to%20a (2019). Accessed 21 October 2020.
8. S. Brown, M. Clastre, V. Courdavault, S. E. O'Connor, De novo production of the plant-derived alkaloid strictosidine in yeast. *Proc. Natl. Acad. Sci. U.S.A.* **112**, 3205–3210 (2015).
9. F. Geu-Flores *et al.*, An alternative route to cyclic terpenes by reductive cyclization in iridoid biosynthesis. *Nature* **492**, 138–142 (2012).
10. C. Ignea *et al.*, Orthogonal monoterpenoid biosynthesis in yeast constructed on an isomeric substrate. *Nat. Commun.* **10**, 3799 (2019).
11. X. Luo *et al.*, Complete biosynthesis of cannabinoids and their unnatural analogues in yeast. *Nature* **567**, 123–126 (2019).
12. K. Miettinen *et al.*, The seco-iridoid pathway from Catharanthus roseus. *Nat. Commun.* **5**, 3606 (2014).
13. P. M. Dewick, *Medicinal Natural Products: A Biosynthetic Approach* (ed. 3, Wiley, 2009).
14. C. Ignea, M. Pontini, M. E. Maffei, A. M. Makris, S. C. Kampranis, Engineering monoterpene production in yeast using a synthetic dominant negative geranyl diphosphate synthase. *ACS Synth. Biol.* **3**, 298–306 (2014).
15. B. Peng, L. K. Nielsen, S. C. Kampranis, C. E. Vickers, Engineered protein degradation of farnesyl pyrophosphate synthase is an effective regulatory mechanism to increase monoterpene production in Saccharomyces cerevisiae. *Metab. Eng.* **47**, 83–93 (2018).
16. M. D. Leavell, D. J. McPhee, C. J. Paddon, Developing fermentative terpenoid production for commercial usage. *Curr. Opin. Biotechnol.* **37**, 114–119 (2016).
17. C. J. Paddon *et al.*, High-level semi-synthetic production of the potent antimalarial artemisinin. *Nature* **496**, 528–532 (2013).
18. A. L. Meadows *et al.*, Rewriting yeast central carbon metabolism for industrial isoprenoid production. *Nature* **537**, 694–697 (2016).
19. S. Cheng *et al.*, Orthogonal engineering of biosynthetic pathway for efficient production of limonene in Saccharomyces cerevisiae. *ACS Synth. Biol.* **8**, 968–975 (2019).
20. G. Z. Jiang *et al.*, Manipulation of GES and ERG20 for geraniol overproduction in Saccharomyces cerevisiae. *Metab. Eng.* **41**, 57–66 (2017).
21. A. A. Sibirny, Yeast peroxisomes: Structure, functions and biotechnological opportunities. *FEMS Yeast Res.* **16**, fow038 (2016).
22. R. Saraya, M. Veenhuis, I. J. van der Klei, Peroxisomes as dynamic organelles: Peroxisome abundance in yeast. *FEBS J.* **277**, 3279–3288 (2010).
23. Y. J. Zhou *et al.*, Harnessing yeast peroxisomes for biosynthesis of fatty-acid-derived biofuels and chemicals with relieved side-pathway competition. *J. Am. Chem. Soc.* **138**, 15368–15377 (2016).
24. J. Sheng, J. Stevens, X. Feng, Pathway compartmentalization in peroxisome of Saccharomyces cerevisiae to produce versatile medium chain fatty alcohols. *Sci. Rep.* **6**, 26884 (2016).
25. V. D. Antonenkov, S. Mindthoff, S. Grunau, R. Erdmann, J. K. Hiltunen, An involvement of yeast peroxisomal channels in transmembrane transfer of glyoxylate cycle intermediates. *Int. J. Biochem. Cell Biol.* **41**, 2546–2554 (2009).
26. S. Lajus *et al.*, Engineering the yeast Yarrowia lipolytica for production of polylactic acid homopolymer. *Front. Bioeng. Biotechnol.* **8**, 954 (2020).
27. R. Breitling, O. Sharif, M. L. Hartman, S. K. Krisans, Loss of compartmentalization causes misregulation of lysine biosynthesis in peroxisome-deficient yeast cells. *Eukaryot. Cell* **1**, 978–986 (2002).
28. D. A. Yee *et al.*, Engineered mitochondrial production of monoterpenes in Saccharomyces cerevisiae. *Metab. Eng.* **55**, 76–84 (2019).
29. P. S. Grewal, J. A. Samson, J. J. Baker, B. Choi, J. E. Dueber, Peroxisome compartmentalization of a toxic enzyme improves alkaloid production. *Nat. Chem. Biol.*, 10.1038/s41589-020-00668-4 (2020).
30. L. Gidijala *et al.*, An engineered yeast efficiently secreting penicillin. *PLoS One* **4**, e8317 (2009).
31. Y. Poirier, N. Erard, J. MacDonald-Comber Petétot, Synthesis of polyhydroxyalkanoate in the peroxisome of Pichia pastoris. *FEMS Microbiol. Lett.* **207**, 97–102 (2002).
32. D. Hoepfner, D. Schildknegt, I. Braakman, P. Philippsen, H. F. Tabak, Contribution of the endoplasmic reticulum to peroxisome formation. *Cell* **122**, 85–95 (2005).
33. G. Agrawal, S. Subramani, Emerging role of the endoplasmic reticulum in peroxisome biogenesis. *Front. Physiol.* **4**, 286 (2013).
34. B. Knoblach *et al.*, An ER-peroxisome tether exerts peroxisome population control in yeast. *EMBO J.* **32**, 2439–2453 (2013).
35. R. Ciriminna, M. Lomeli-Rodriguez, P. Demma Carà, J. A. Lopez-Sanchez, M. Pagliaro, Limonene: A versatile chemical of the bioeconomy. *Chem. Commun. (Camb.)* **50**, 15288–15296 (2014).
36. N. I. Tracy, D. Chen, D. W. Crunkleton, G. L. Price, Hydrogenated monoterpenes as diesel fuel additives. *Fuel* **88**, 2238–2240 (2009).
37. C. Ignea *et al.*, Synthesis of 11-carbon terpenoids in yeast using protein and metabolic engineering. *Nat. Chem. Biol.* **14**, 1090–1098 (2018).
38. R. Croteau, Biosynthesis and catabolism of monoterpenoids. *Chem. Rev.* **87**, 929–954 (1987).
39. B. Peng *et al.*, A squalene synthase protein degradation method for improved sesquiterpene production in Saccharomyces cerevisiae. *Metab. Eng.* **39**, 209–219 (2017).
40. A. Bhataya, C. Schmidt-Dannert, P. C. Lee, Metabolic engineering of Pichia pastoris X-33 for lycopene production. *Process Biochem.* **44**, 1095–1102 (2009).
41. C. Zhang, M. Li, G. R. Zhao, W. Lu, Harnessing yeast peroxisomes and cytosol acetyl-CoA for sesquiterpene α-humulene production. *J. Agric. Food Chem.* **68**, 1382–1389 (2020).
42. W. C. DeLoache, Z. N. Russ, J. E. Dueber, Towards repurposing the yeast peroxisome for compartmentalizing heterologous metabolic pathways. *Nat. Commun.* **7**, 11152 (2016).
43. P. J. Espenshade, A. L. Hughes, Regulation of sterol synthesis in eukaryotes. *Annu. Rev. Genet.* **41**, 401–427 (2007).
44. P. J. Westfall *et al.*, Production of amorphadiene in yeast, and its conversion to dihydroartemisinic acid, precursor to the antimalarial agent artemisinin. *Proc. Natl. Acad. Sci. U.S.A.* **109**, E111–E118 (2012).
45. X. Cao, S. Yang, C. Cao, Y. J. Zhou, Harnessing sub-organelle metabolism for biosynthesis of isoprenoids in yeast. *Synth. Syst. Biotechnol.* **5**, 179–186 (2020).
46. T. C. R. Brennan, C. D. Turner, J. O. Krömer, L. K. Nielsen, Alleviating monoterpene toxicity using a two-phase extractive fermentation for the bioproduction of jet fuel mixtures in Saccharomyces cerevisiae. *Biotechnol. Bioeng.* **109**, 2513–2522 (2012).
47. B. Ribeiro, P. Shapira, Anticipating governance challenges in synthetic biology: Insights from biosynthetic menthol. *Technol. Forecast. Soc. Change* **139**, 311–320 (2019).
48. J. Lücker *et al.*, Metabolic engineering of monoterpene biosynthesis: Two-step production of (+)-trans-isopiperitenol by tobacco. *Plant J.* **39**, 135–145 (2004).

Dusséaux et al.

49. S. C. Rastogi, S. Heydorn, J. D. Johansen, D. A. Basketter, Fragrance chemicals in domestic and occupational products. *Contact Dermat.* **45**, 221–225 (2001).

50. W. Chen, A. M. Viljoen, Geraniol—A review of a commercially important fragrance material. *S. Afr. J. Bot.* **76**, 643–651 (2010).

51. Y. Iijima, D. R. Gang, E. Fridman, E. Lewinsohn, E. Pichersky, Characterization of geraniol synthase from the peltate glands of sweet basil. *Plant Physiol.* **134**, 370–379 (2004).

52. Market Research Future, Microbial products market size, share, technology growth by 2023, https://www.marketresearchfuture.com/reports/microbial-products-market-765 (2020). Accessed 21 October 2020.

53. G. S. Liu *et al.*, The yeast peroxisome: A dynamic storage depot and subcellular factory for squalene overproduction. *Metab. Eng.* **57**, 151–161 (2020).

54. Y. Ren, S. Liu, G. Jin, X. Yang, Y. J. Zhou, Microbial production of limonene and its derivatives: Achievements and perspectives. *Biotechnol. Adv.* **44**, 107628 (2020).

55. S. H. Kung, S. Lund, A. Murarka, D. McPhee, C. J. Paddon, Approaches and recent developments for the commercial production of semi-synthetic artemisinin. *Front Plant Sci* **9**, 87 (2018).

56. Y. Yoshikuni, J. A. Dietrich, F. F. Nowroozi, P. C. Babbitt, J. D. Keasling, Redesigning enzymes based on adaptive evolution for optimal function in synthetic metabolic pathways. *Chem. Biol.* **15**, 607–618 (2008).

57. F. A. Trikka *et al.*, Iterative carotenogenic screens identify combinations of yeast gene deletions that enhance sclareol production. *Microb. Cell Fact.* **14**, 60 (2015).

58. C. J. Paddon, J. D. Keasling, Semi-synthetic artemisinin: A model for the use of synthetic biology in pharmaceutical development. *Nat. Rev. Microbiol.* **12**, 355–367 (2014).

59. J. C. Farré, S. S. Mahalingam, M. Proietto, S. Subramani, Peroxisome biogenesis, membrane contact sites, and quality control. *EMBO Rep.* **20**, e46864 (2019).

60. A. van der Zand, I. Braakman, H. F. Tabak, Peroxisomal membrane proteins insert into the endoplasmic reticulum. *Mol. Biol. Cell* **21**, 2057–2065 (2010).

61. C. David *et al.*, A combined approach of quantitative interaction proteomics and live-cell imaging reveals a regulatory role for endoplasmic reticulum (ER) reticulon homology proteins in peroxisome biogenesis. *Mol. Cell. Proteomics* **12**, 2408–2425 (2013).

62. W. Runguphan, J. D. Keasling, Metabolic engineering of Saccharomyces cerevisiae for production of fatty acid-derived biofuels and chemicals. *Metab. Eng.* **21**, 103–113 (2014).

63. S. C. Kampranis *et al.*, Rational conversion of substrate and product specificity in a Salvia monoterpene synthase: Structural insights into the evolution of terpene synthase function. *Plant Cell* **19**, 1994–2005 (2007).

64. A. Tsaballa *et al.*, Use of the de novo transcriptome analysis of silver-leaf nightshade (Solanum elaeagnifolium) to identify gene expression changes associated with wounding and terpene biosynthesis. *BMC Genomics* **16**, 504 (2015).

65. H. H. Nour-Eldin, F. Geu-Flores, B. A. Halkier, USER cloning and USER fusion: The ideal cloning techniques for small and big laboratories. *Methods Mol. Biol.* **643**, 185–200 (2010).

66. F. Geu-Flores, H. H. Nour-Eldin, M. T. Nielsen, B. A. Halkier, USER fusion: A rapid and efficient method for simultaneous fusion and cloning of multiple PCR products. *Nucleic Acids Res.* **35**, e55 (2007).

67. M. D. Mikkelsen *et al.*, Microbial production of indolylglucosinolate through engineering of a multi-gene pathway in a versatile yeast expression platform. *Metab. Eng.* **14**, 104–111 (2012).

68. K. G. Vanegas, B. J. Lehka, U. H. Mortensen, SWITCH: A dynamic CRISPR tool for genome engineering and metabolic pathway control for cell factory construction in Saccharomyces cerevisiae. *Microb. Cell Fact.* **16**, 25 (2017).